Heliyon 5 (2019) e02305

Contents lists available at ScienceDirect

Heliyon

journal homepage: www.heliyon.com

Application of diffusion and transition state theories on the carburizing of steel AISI 316 by annealing in uranium carbide powder

Yüksel Sarıkaya [a], Müşerref Önal [a,*], Abdullah Devrim Pekdemir [b]

[a] Ankara University, Faculty of Science, Department of Chemistry, Tandoğan, 06100 Ankara, Turkey
[b] Ankara University, Graduate School of Natural and Applied Sciences, Ankara, Turkey

ARTICLE INFO

Keywords:
Materials science
Physical chemistry
Metals
Materials property
Surface chemistry
Uranium carbide
Transition state theory
Carburizing
Diffusion
AISI 316 steel
Microhardness

ABSTRACT

The steel specimens were tempered in contact with uranium carbide powder by sodium bonding at 500, 600, 700, and 800 °C for 1000h. Carburizing zone of the specimens was determined by measuring of microhardness which is taken as a kinetic variable instead of the corresponding carbon content. Arrhenius equation was determined for the diffusion of carbon atoms in the steel by using the solution of Fick's second law. Temperature dependency of the activation enthalpy, Gibbs energy, and entropy was calculated from the transition state theory by an assumption that the carburizing occurs over an activated complex. Kinetic and thermodynamic for formation an activated complex were discussed depending on the obtained numerical values.

1. Introduction

Fuels and their cladding are the main materials for nuclear reactors. Plutonium-uranium oxide, $(Pu_xU_{1-x})O_2$, or plutonium-uranium carbide, $(Pu_xU_{1-x})C$, has been used to be nuclear fuel. Carbide fuel is obtained by the vacuum carbothermic reaction from oxide fuel [1]. Cladding for the fuel tips are made of usually austenitic stainless steels due to their excellent mechanical and physicochemical properties [2, 3]. These properties such as corrosion resistance, hardness, ductility, elongation at rupture, wear resistance, fracture strength, fatigue strength, tensile strength, and yield strength change by the physicochemical interactions with the fuels at the working temperature of the reactors [4, 5].

Chemical compatibility between carbide fuel and cladding is more than those oxide one. Namely, chemical effect of an oxide fuel and its fission products on cladding is a great extent, whereas a carbide fuel limited [6]. Nevertheless, preparation and using a carbide fuel are much more difficult than those oxide one.

Diffusion of carbon atoms into a steel from a carbonaceous medium in solid, liquid or gas phase is known as carburizing. Carbon content decreased from the surface to interior of the steel. The carburized zone and interior core in the steel remain integrally bonded. The effect of carburizing in several carbonaceous mediums on the mechanical and physicochemical properties of steels have been investigated [7, 8, 9, 10].

Carburizing process have been clearly examined with out-of-pin annealing test. This test realized between cladding materials and fuels as well as their fission product is very important to prevent the most dangerous accidents would be arisen from the core of nuclear reactors. Since they have similar chemical properties, a uranium carbide powder has been used instead of the real carbide fuel by the test [11, 12]. Distribution and depth of the carburized zone in the steel have been determined by the measurement of carbon content or microhardness [13, 14, 15, 16]. Since the hardness changes depending on the carbon content in the steel, there is a direct correlation between the microhardness and carbon content profiles which was experimentally proved [12, 13, 14, 15]. Microscopy also has been used to examine the carburizing [17, 18, 19]. Carbon content or microhardness profiles change depending on the annealing temperature and its time as well as the rate of the cooling process [20, 21, 22]. Metal-carbon nanostructures such as $Cr_{23}C_6$ were found on the contact surface and carburized zone of the steel [18]. Several attempts have been made to mathematical evaluate of the profiles [23, 24]. However, kinetic and thermodynamic explanations have not been adequate to understand the theoretical nature of the carburizing [20, 21, 22]. So, the objective and the novelty of the present study respectively are to examine the high temperature carburizing of a steel in

* Corresponding author.
E-mail address: onal@science.ankara.edu.tr (M. Önal).

https://doi.org/10.1016/j.heliyon.2019.e02305
Received 20 December 2018; Received in revised form 19 April 2019; Accepted 9 August 2019

contact with a uranium carbide powder starting from microhardness profiles and firstly using the combination of diffusion and transition state theories for the kinetic calculations.

2. Materials and methods

2.1. Materials

Austenitic stainless steel AISI 316 and a uranium carbide powder were used as a cladding material and carbon medium, respectively [6]. Chemical composition of the steel (mass %) is: Fe, 58.82; Cr, 17.00; Ni, 13.25; Mo, 8.20; Mn, 1.70; Si, 0.45; P, 0.23; Co, 0.14; C, 0.05; Ti, 0.05; Te + Nb, 0.05; N, 0.03; S, 0.02; and Al, 0.01. Chemical composition (mass %) of the uranium carbide powder is: U, 95.016; C (in UC), 4.726; C (free graphite), 0.034; O, 0.170; and N, 0.050.

2.2. Experimental

Cladding specimens were die-pressed from the steel received in sheet-form with the thickness of 1mm. They were annealed in vacuum at 1050 °C for 30 min to remove fin-grained surface zone by the preparation. Carburizing of the specimens was realized by the out-of-pile annealing tests. Because of the uranium carbide powder is greatly pyrophoric, the preparation procedure was carried out under a pure argon atmosphere in a glove box.

Special prepared four steel capsules each having four parallel strip specimens were filled with the uranium carbide powder and then adding a sufficient amount liquid sodium tightly enclosed. The steel capsules taken out of the glove box were encapsulated again by evacuating silica capsules. Each capsule was heated in a muffle oven at various temperatures of 500, 600, 700, and 800 °C for 1000h. The capsules stand to cooling in the oven up to room temperature and then the carburized specimens were taken out by cut of them. After completion of the elementary treatments the microhardness gradients from the contact surface to the interior of the specimens were measured at room temperature with a Leitz Durimet machine [6].

3. Results and discussion

3.1. Kinetics for carburizing

Carburized zone of the steel specimens annealed at the different temperatures is seen from the microhardness profiles which are given in Fig. 1a, b, c, and d. These profiles revealed that the microhardness at the contact surface (h_s) and maximum depth (x_{max}) for the carburized zone greatly change depending on the annealing temperature. The h_s and x_{max} values which are taken from the profiles and given in Table 1.

Because the hardening is due to the diffusion of carbon atoms in the steel the microhardness would be taken as a kinetic variable instead of the corresponding carbon content. The shape of the microhardness pro-

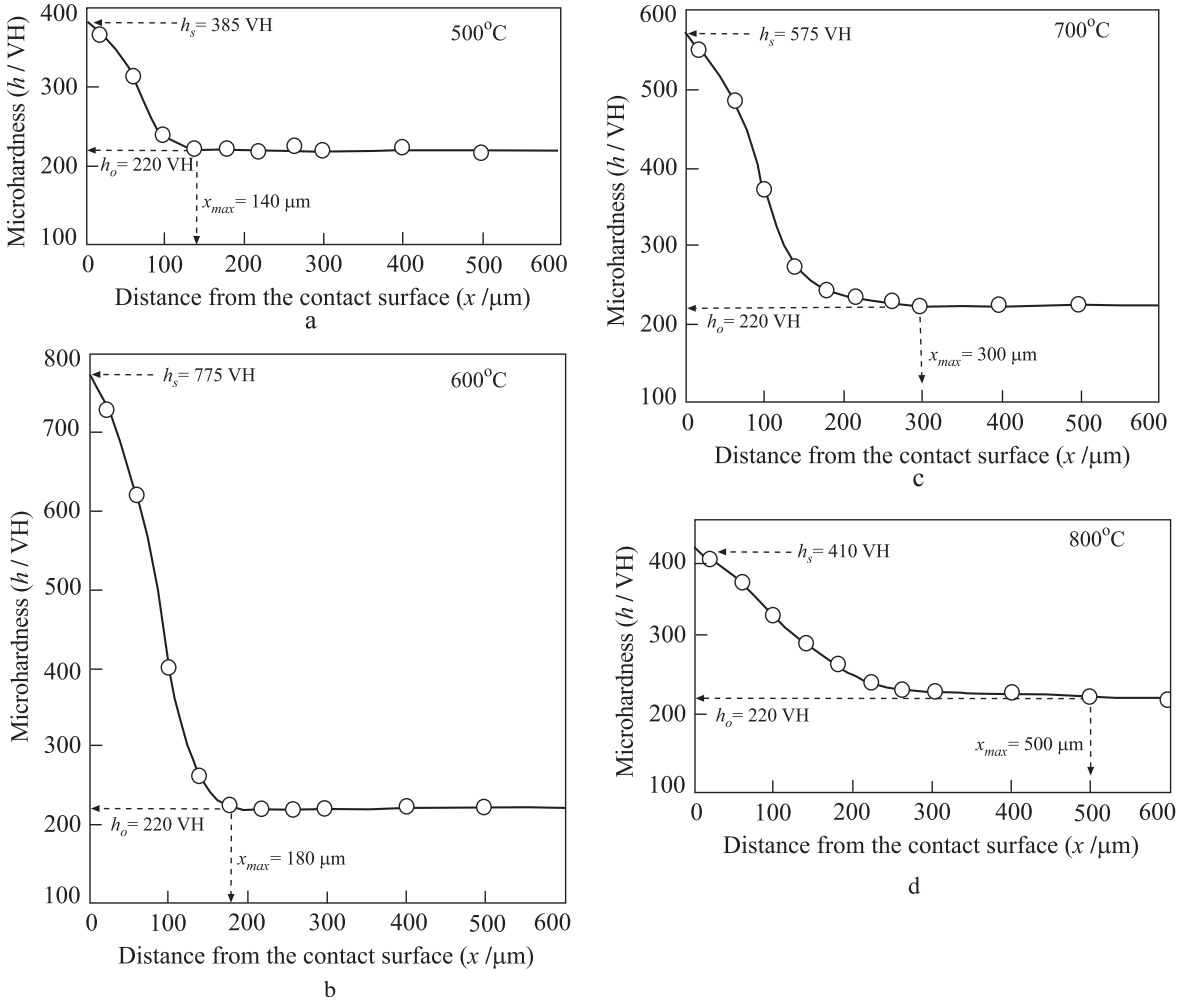

Fig. 1. (a) Microhardness profile at 500 °C temperature (b) Microhardness profile at 600 °C temperature (c) Microhardness profile at 700 °C temperature (d) Microhardness profile at 800 °C temperature (h_o: microhardness of the untreated steel, h_s: maximum microhardness at nearest the contact surface, x_{max}: maximum thickness of the carburized zone).

files appeared to verify the Fick's diffusion laws. Thus, the equation for the microhardness profiles and mean square depth, $<x^2>$ are respectively derived from the approximate solution of Fick's second law in the following forms [22, 23, 24]:

$$H = \frac{h - h_0}{h_s - h_0} = \frac{1}{2(\pi Dt)^{1/2}} \exp\left(-\frac{x^2}{4Dt}\right) \quad (1)$$

$$< x^2 > = 2Dt \quad (2)$$

where h_s is the maximum microhardness, $h_o = 220$ HV is the minimum microhardness for the uncarburized steel, h is the microhardness at any depth in the carburized zone, H is defined to be relative microhardness, D is the diffusion coefficient which depends only on temperature, x is any depth of the carburized zone and $t = 1000$h is the constant annealing time. These relationships are respectively known as parabolic and linear law equation for diffusion.

The ln$H$ against x^2 plots which are straight lines as seen in Fig. 2 indicated that the microhardness profiles obey Eq. (1). Diffusion coefficients were obtained from the slope of the straight line and listed in Table 1. The plot of the ln$D$ against $1/T$ is a straight line as seen in Fig. 3 obeys the Arrhenius equation in the following form,

$$\ln D = \ln D_0 - E^{\#}/RT \quad (3)$$

where D_0 is called to be a frequency factor or pre-exponential constant, $E^{\#}$ is the energy of activation, T is the absolute carburizing temperature, and $R = 8.314$ J mol^{-1} K^{-1} is the gas constant. The values of $E^{\#} = 34910$ J mol^{-1} and $D_0 = 6.66 \times 10^{-14}$ m^2 s^{-1} were respectively calculated from the slope and intercept of the straight line in Fig. 3. Accordingly, temperature dependency of the diffusion coefficient can be written in exponential form given as follows:

$$D = 6.66 \times 10^{-14} \exp(-34910/RT) \quad (4)$$

The root mean square depth, $<x^2>^{1/2}$ value of the each temperature was calculated from Eq. (2) and listed Table 1. Their temperature dependence is represented in Fig. 4. The $<x^2>^{1/2}$ is much lower than the corresponding x_{max}. The functional increase of the x_{max} and $<x^2>^{1/2}$ show that the carburized zone extended to inside steel by increasing the annealing temperature.

Several equations to get along with each others in the experimental errors reported by many authors for the carburizing of similar alloys. For example, theoretical carbon content profiles for the carburizing of a steel at a temperature for different times were obtained by using a mathematical model derived from the solution of Fick's second law and compered experimental ones [21]. Carbon content as well as microhardness profiles which are determined depending on the temperature at a constant time or vice versa have been used to evaluate the kinetic parameters as mentioned above [18, 20]. The carburized layer thickness, x, has been used instead of the root mean square distance, $<x^2>^{1/2}$, to calculate the diffusion coefficient from Eq. (2) in several studies [23]. Also, layer thickness is directly used in Arrhenius equation instead of the diffusion coefficient [18, 20, 25].

Table 1
The maximum microhardness (h_s), maximum distance from the contact surface (x_{max}), diffusion coefficient (D), root mean square distance ($<x^2>^{1/2}$), and the equilibrium constant ($K^{\#}$) for the carburizing at different temperatures.

T/K	$(1/T)$/ 10^{-3}K^{-1}	h_s/ VH	x_{max}/ μm	D/ 10^{-16}m^{2}s^{-1}	$<x^2>^{1/2}$/ μm	$K^{\#}/10^{-29}$ m^2
773	1.2937	385	140	3.234	48	2.020
873	1.1455	775	180	4.721	58	2.590
973	1.0277	575	300	8.170	77	4.008
1073	0.9320	410	500	30.193	104	13.499

3.2. Activation thermodynamics for the carburizing

Transition state theory (TST) was applied to the carburizing by supposing the $Cr_{23}C_6$ nanostructure acts as an activated complex (AC). According to TST a chemical equilibrium exists between the $Cr_{23}C_6$ and their atoms in the following schematic form:

$$\text{steel} + \text{UC} \leftrightarrows [\text{AC}]^{\#} \rightarrow \text{carbon transfer} \quad (5)$$

The forward decomposition of the activated complex given in Eq. (5) causes the diffusion of carbon atoms into the steels. In contrary, during the backward decomposition forms uranium carbide powder again. The forward and backward rates depend on temperature and its change with time. The forward rates would be taken as the carburizing rate.

All of the thermodynamic relations are valid for the equilibrium between reactant and activated complex not fully carburized. Eyring equation which is derived from the TST for this equilibrium would be written in the following form [22]:

$$K^{\#} = Dh/k_BT \quad (6)$$

where $k_B = 1.38 \times 10^{-23}$ J K^{-1} is the Boltzmann constant, $h = 6.62 \times 10^{-34}$ J s is the Planck constant, and $K^{\#}$ is the equilibrium constant for the formation reaction of the activated complex. The $K^{\#}$ value of the each temperature is calculated and listed in Table 1.

The temperature dependence of the activation enthalpy ($\Delta H^{\#}$) can be evaluated by inserting Arrhenius ($d\ln D/dT = E^{\#}/RT^2$) and van't Hoff ($d\ln K^{\#}/dT = \Delta H^{\#}/RT^2$) relations in the temperature derivative of the logarithmic Eyring equation in the following form:

$$\ln K^{\#} = \ln D + \ln h - \ln k_B - \ln T \quad (7)$$

$$d\ln K^{\#}/dT = d\ln D/dT - 1/T \quad (8)$$

$$\Delta H^{\#}/RT^2 = E^{\#}/RT^2 - 1/T \quad (9)$$

$$\Delta H^{\#} = E^{\#} - RT \quad (10)$$

$$\Delta H^{\#} = 34910 - 8.314T \quad (11)$$

According to this equation $\Delta H^{\#} > 0$ between 500-800 °C and the

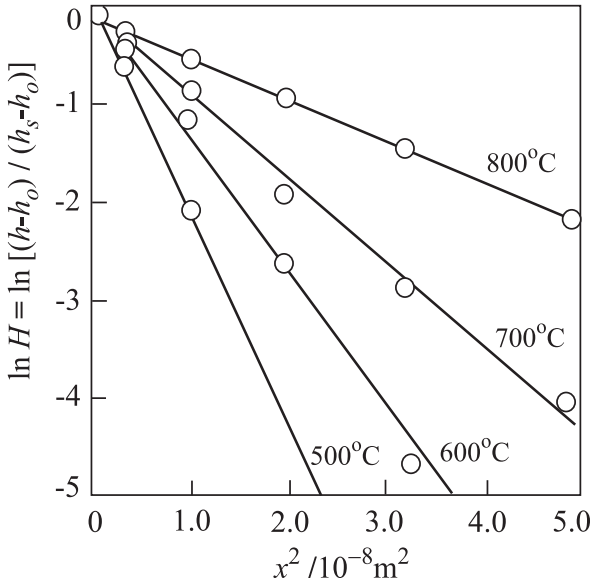

Fig. 2. The plot of the natural logarithm of relative microhardness (ln$H$) against the square distance (x^2) from the contact surface for the each carburizing temperature.

formation of the AC is endothermic.

Change in heat capacity ($\Delta C_p^{\#}$) by the formation of the AC is found by using Kirchhoff's equation as follows:

$$\Delta C_p^{\#} = d\Delta H^{\#}/dT = -8.314 \mathrm{JK}^{-1}\mathrm{mol}^{-1} \quad (12)$$

This negative value indicated that the total vibration modes of atoms decreased during the formation of the activated complex.

Variation of the $\ln K^{\#}$ with the carburizing temperature between 500 and 800 °C was calculated from the integration of the van't Hoff relation in the following form:

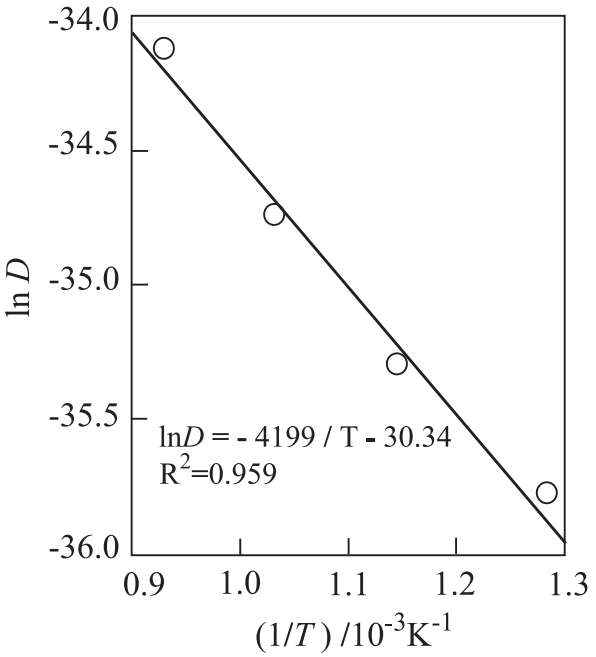

Fig. 3. The plot of the natural logarithm of diffusion coefficient (ln$D$) against the reciprocal of the temperature ($1/T$) for the carburizing.

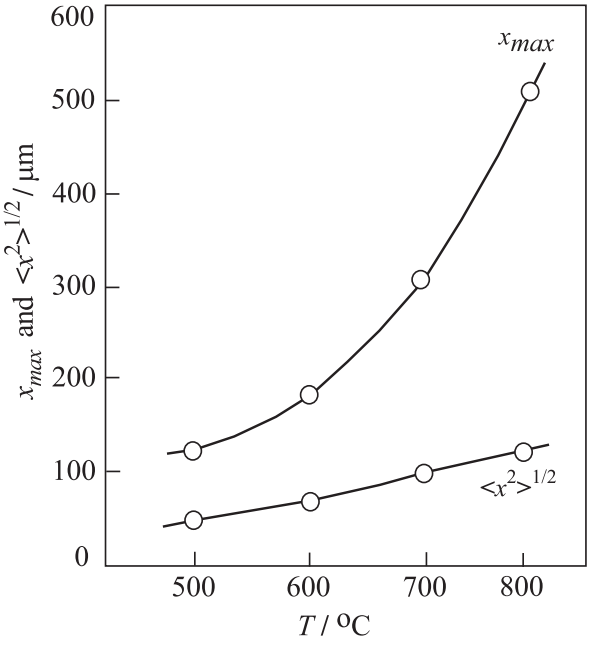

Fig. 4. The plot of the maximum distance (x_{max}) and root mean square distance ($<x^2>^{1/2}$) from the contact surface against the carburizing temperature (T).

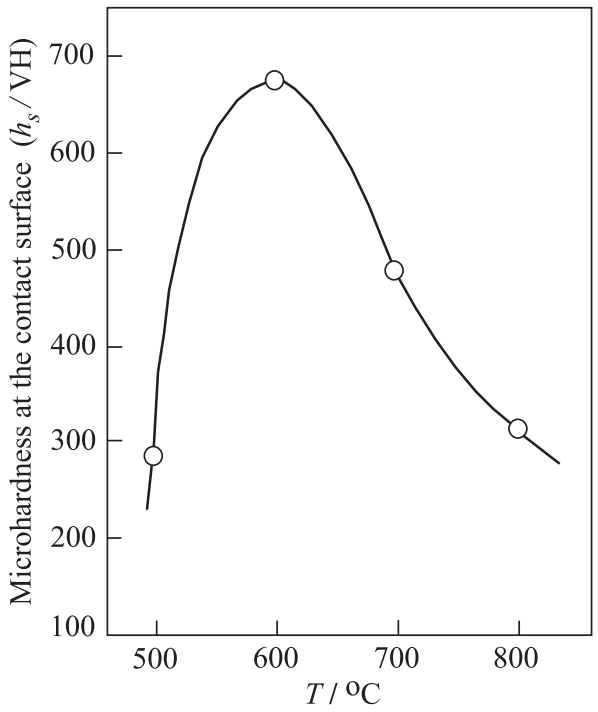

Fig. 5. The plot of the maximum microhardness (h_s) against the carburizing temperature (T).

$$\ln K^{\#} = \int (\Delta H^{\#}/RT^2)dT = -4199/T - \ln T - 54 \quad (13)$$

where -54 is an integral constant that is the arithmetic mean of the values calculated for each temperature by using the corresponding $K^{\#}$ values.

Variation of the Gibbs free energy ($\Delta G^{\#}$) and entropy ($\Delta S^{\#}$) with the temperature were respectively calculated using the basic thermodynamic equations in the following forms:

$$\Delta G^{\#} = -RT \ln K^{\#} = 34910 + 8.314\, T \ln T + 449T \quad (14)$$

$$\Delta S^{\#} = -d\Delta G^{\#}/dT = -440.6 - 8.314 \ln T \quad (15)$$

As a result, the positive value of $\Delta G^{\#}$ and the negative value of $\Delta S^{\#}$ increase with the increasing of the carburizing temperature between 500 and 800 °C. However, the spontaneous diffusion of carbon atoms into steel reveals that the total Gibbs energy (ΔG) could be negative by the carburizing.

The positive value of the $\Delta G^{\#}$ indicated that the activated complex does not form spontaneously. But it is carried out mandatory by given continuous energy from surrounding as similar as the formation of the ozone layer in the atmosphere. Also, the negative value of $\Delta C_p^{\#}$ and $\Delta S^{\#}$ is verified the formation of $Cr_{23}C_6$ nanostructure as an activated complex [7]. Because of decrease in the number of vibration modes and disorder during the formation an activated complex by the bonding of many atoms causes the lowering in the heat capacity and entropy, respectively.

The h_s against T plot has a maximum as seen in Fig. 5. The change in the kinetic parameters in an opposite way before and after 600 °C would be the reason of the maximum. This maximum would be originated from the increasing of the forward decomposition rate of the activated complex before 600 °C and after the backward rate.

4. Conclusions

Fick's second law and transition state theory were firstly applied to calculate kinetic parameters for high temperature carburizing of a steel in a uranium carbide powder. Microhardness profile for the carburized zones was used in the calculations instead of the carbon content profile.

The kinetic and thermodynamic results indicated that the transfer of carbon atom from a solid phase to the steel would be over an activated complex. The proposed calculation method would be used also to examine the carburizing of the other alloys and pure metals by tempering in contact with an inorganic and organic carbon medium.

Declarations

Author contribution statement

Yüksel Sarıkaya: Conceived and designed the experiments; Performed the experiments.

Müşerref Önal: Analyzed and interpreted the data; Contributed reagents, materials, analysis tools or data; Wrote the paper.

A.Devrim Pekdemir: Analyzed and interpreted the data; Contributed reagents, materials, analysis tools or data.

Funding statement

This work was supported by Ankara University Research Fund (Project No: 16L0430013).

Competing interest statement

The authors declare no conflict of interest.

Additional information

No additional information is available for this paper.

Acknowledgements

The authors thank to Research Center Karlsruhe for the experimental facilities.

References

[1] S. Majumdar, A.K. Sengupta, H.S. Kamath, Fabrication, characterization and property evaluation of mixed carbide fuels for a test Fast Breeder Reactor, J. Nucl. Mater. 352 (2006) 165–173.

[2] K. Tokaji, K. Kohyama, M. Akita, Fatigue behaviour and fracture mechanism of a 316 stainless steel hardened by carburizing, Int. J. Fatigue 26 (2004) 543–551.

[3] X. Xia, K. Idemitsu, T. Arima, Y. Inagki, T. Ishidera, S. Kurosawa, K. Iijima, H. Sato, Corrosion of carbon steel in compacted bentonite and its effect on neptunium diffusion under reducing condition, Appl. Clay Sci. 28 (2005) 89–100.

[4] W. Zhang, K. Fang, Y. Hu, S. Wang, X. Wang, Effect of machining-induced surface residual stress on initiation of stress corrosion cracking in 316 austenitic stainless steel, Corros. Sci. 108 (2016) 173–184.

[5] W. Juan, L. Yajiang, M. Haijum, Diffusion bonding of Fe- 28 Al (Cr) alloy with low-carbon steel in vacuum, Vacuum 80 (2006) 426–431.

[6] O. Götzmann, P. Hofmann, Y. Sarıkaya, Mechanical Properties of Cladding Materials after Annealing with Carbide Fuels, Fuel and Materials Specialist Meeting of the Coordinating Group on Gas Cooled Fast Reactor Development, Würenlingen, 1973.

[7] B. Kurt, N. Orhan, A. Hasçalık, Effect of high heating and cooling rate on interface of diffusion bonded gray cost iron to medium carbon steel, Mater. Des. 28 (2007) 2229–2233.

[8] S. Wang, Y. Hu, K. Fang, W. Zhang, X. Wang, Effect of surface on the corrosion behaviour of 316 austenitic stainless steel in simulated PWR water, Corros. Sci. 126 (2017) 104–120.

[9] M.G. Fillabi, A. Simchi, A.H. Kokabi, Effect of iron particle size on the diffusion bonding of Fe-5%Cu powder compact to wrought carbon steels, Mater. Des. 29 (2008) 411–417.

[10] D. Götzmann, R.W. Ohse, Fuel cladding compatibility of stainless steel with gas and sodium bonded uranium- plutonium carbide fuels, EUR- 4897e, European-American Nuclear Data Commitee, 1972.

[11] W.E. Stumpf, O. Götzmann, Room temperature mechanical properties and precipitation behavior of Steer X8CrNiMoVNb 1613 (4988), Incoloy 800 and Inconel 718 after annealing in contact with UC at 600°C to 800°C, Institut für Material- und Festkörperforschung, Projekt Schneller Brüter, KFK 1384, 1971, Kernforschungszentrum Karlsruhe, 1971.

[12] A. Pertek, M. Kulka, Two- step treatment carburizing followed by boriding on medium- carbon steel, Surf. Coat. Technol. 173 (2003) 309–314.

[13] C.S. Li, Y.S. Yang, A glass based coating for enhancing anti-coking and anti-carburizing abilities of heat- resistant steel HP, Surf. Coat. Technol. 185 (2004) 68–73.

[14] A. Pertek, M. Kulka, Characterization of complex (B+C) diffusion layers formed on chromium and nickel- based low- carbon steel, Appl. Surf. Sci. 202 (2002) 252–260.

[15] M. Kulka, A. Pertek, Characterization of complex (B+C+N) diffusion layers formed on chromium and nickel- based low- carbon steel, Appl. Surf. Sci. 218 (2003) 113–122.

[16] M. Akita, K. Tokaji, Effect of carburizing on notch fatigue behavior in AISI 316 austenitic stainless steel, Surf. Coat. Technol. 200 (2006) 6073–6078.

[17] J. Yao, Q. Zhang, M. Gao, W. Zhang, Microstructure and wear property of carbon nanotube carburizing carbon steel by laser surface remelting, Appl. Surf. Sci. 254 (2008) 7092–7097.

[18] M.F. Yan, Study on absorption and transport of carbon in steel during gas carburizing with rare- earth addition, Mater. Chem. Phys. 70 (2001) 242–244.

[19] Y. Sun, Kinetics of low temperature plasma carburizing of austenitic stainless steels, J. Mater. Process. Technol. 168 (2005) 189–194.

[20] I. Jauhari, S. Rozali, N.R.N. Masdek, O. Hiroyuki, Surface properties and activation energy analysis for super plastic carburizing of duplex stainless steel, Mater. Sci. Eng. A 466 (2007) 230–234.

[21] H. Jiménez, M.H. Staia, E.S. Puchi, Mathematical modeling of a carburizing process of a SAE 8620H steel, Surf. Coat. Technol. 120–121 (1999) 358–365.

[22] A. Sugianto, M. Narazaki, M. Kogawara, A. Shirayori, S.-Y. Kim, S. Kubota, Numerical simulation and experimental verification of carburizing- quenching process of SCr420H steel helical gear, J. Mater. Process. Technol. 209 (2009) 3597–3609.

[23] N.W. Ahamad, I. Jahuri, S.A.A. Azis, N.H.A. Azis, Kinetics of carburizing of duplex stainless steel (DSS) by super plastic compression at different strain rates, Mater. Sci. Eng. A 527 (2010) 4257–4261.

[24] Y. Sarıkaya, M. Önal, High temperature carburizing of a stainless steel with uranium carbide, J. Alloy. Comp. 542 (2012) 253.

[25] C.J. Scheuer, R.P. Cardoso, M. Mafra, S.F. Brunatto, AISI 420 martensitic stainless steel low-temperature plasma assisted carburizing kinetics, Surf. Coat. Technol. 214 (2013) 30–37.